haematologica
Journal of the Ferrata Storti Foundation

Irradiated CD19 chimeric antigen receptor YTS cells retain antitumor activity and offer a scalable alternative to autologous CAR-T therapy

by Hanan Jaber, Anas Abu khalaf, Lola Weiss, Itay Cohen, Natali Bannoura, Tamara Osaili, Ortal Maximov, Abigael Eva Chaouat, Mark Kournos, Adi Tabib, Dror Mevorach, Yarden Engel, Michael Berger, Ofer Mandelboim and Shlomo Elias

Received: November 4, 2025.
Accepted: July 27, 2026.

Citation: Hanan Jaber, Anas Abu khalaf, Lola Weiss, Itay Cohen, Natali Bannoura, Tamara Osaili, Ortal Maximov, Abigael Eva Chaouat, Mark Kournos, Adi Tabib, Dror Mevorach, Yarden Engel, Michael Berger, Ofer Mandelboim and Shlomo Elias. Irradiated CD19 chimeric antigen receptor YTS cells retain antitumor activity and offer a scalable alternative to autologous CAR-T therapy. Haematologica. 2026 Aug 13. doi: 10.3324/haematol.2025.300165 [Epub ahead of print]

Publisher's Disclaimer.
E-publishing ahead of print is increasingly important for the rapid dissemination of science. Haematologica is, therefore, E-publishing PDF files of an early version of manuscripts that have completed a regular peer review and have been accepted for publication.
E-publishing of this PDF file has been approved by the authors.
After having E-published Ahead of Print, manuscripts will then undergo technical and English editing, typesetting, proof correction and be presented for the authors' final approval, the final version of the manuscript will then appear in a regular issue of the journal.
All legal disclaimers that apply to the journal also pertain to this production process.

Irradiated CD19 chimeric antigen receptor YTS cells retain antitumor activity and offer a scalable alternative to autologous CAR-T therapy

Hanan Jaber[1,2*], Anas Abu khalaf[1,2*], Lola Weiss[1], Itay Cohen[1,2], Natali Bannoura[1,2], Tamara Osaili,[1,2] Ortal Maximov,[1,2] Abigael Eva Chaouat [1,2], Mark Kournos[2], Adi Tabib[3], Dror Mevorach[3], Yarden Engel[2], Michael Berger[2], Ofer Mandelboim[2] and Shlomo Elias[1,2]

[1] Department of Bone Marrow Transplantation and Cancer Immunotherapy, Hadassah Medical Center, Faculty of Medicine, Hebrew University of Jerusalem, Jerusalem, Israel

[2] The Lautenberg Center for General and Tumor Immunology, Department of Immunology and Cancer Research, Institute for Medical Research Israel Canada (IMRIC), Hebrew University-Hadassah Medical School, Jerusalem Israel.

[3] Institute of Rheumatology-Immunology-Allergology and Department of Medicine, Hadassah Medical Center, Faculty of Medicine, Hebrew University of Jerusalem, Jerusalem, Israel

[*] These authors contributed equally

Running title: Engineered YTS cells as a cellular therapy

Keywords: YTS, NK, CAR-CD19, immunotherapy

Details of corresponding authors: Correspondence should be sent to Shlomo Elias selias@hadassah.org.il, Tel: 972-2-6757515, Fax: 972-2-6757227

Competing interests: The authors declare that they have no competing interests.

Author Contributions

HJ performed most of the *in vitro* experiments. AAK performed the mice experiments and other experiments. LW assisted with mouse experiments. IC, NB, AEC, OM (Maximov) and AT performed or assisted to experiments. MK generated the 2B4 knockout cells. AT and DM assisted with dendritic cell experiments. YE and MB provided and assisted with melanoma cell lines and related analyses. OM (Mandelboim) and SE conceptualized the study, SE supervised the research. HJ and SE wrote and edited the manuscript. All authors provided critical feedback, and approved the final version of the manuscript.

Data Sharing Statement

All data generated or analyzed during this study are included in this published article and its supplementary information files. Any remaining raw data or protocols are available from the corresponding author upon reasonable request.

Conflict of interest statement

H.J., A.A.K., O.M., and S.E. are listed as inventors on a patent application related to the use of engineered YTS cells for immunotherapy (PCT Patent Application No. PCT/IL2024/050118). The remaining authors declare no competing financial interests.

Acknowledgments

We thank Shlomit Kfir-Erenfeld and Natalie Asherie from the Department of Bone Marrow transplantation at Hadassah Medical Center for assistance in the CAR-T production. We thank Dana G. Wolf and Esther Oiknine-Djian from the Clinical Virology Unit, Department of Clinical Microbiology and Infectious Diseases, for their assistance with the EBV experiments.

We thank Zhanna Yekhtin for assistance with the mice experiments. ChatGPT (OpenAI, San Francisco, CA, USA) was used to improve the language and readability of the manuscript. The authors reviewed and edited the content as needed and take full responsibility for the final text.

Funding

SE is supported by Hadassah "OFEK" research fund, ASH global research award, ISF grant (2873/23), Israel Society of Hematology and Transfusion Medicine, and grant of the Ministry of Innovation, Science and Technology (0007868). HJ is supported by the Golda Meir Endowment Fund for postdoctoral fellowship. Ofer Mandelboim is supported by: The Israel Science Foundation grant 3042/22, grant 442/18 and grant 619/23; The German-Israeli Foundation for Scientific Research and Development Grant 1412-414.13/2017; The Israel Innovation Authority grant 75934; The ICRF professorship; The Yissum grant 220318; and The MOST-DKFZ grant 3-14931 and grant 3 14930. The funders had no role in the study design, data collection, analysis, interpretation of data, writing of the manuscript, or the decision to submit the article for publication.

Abstract

Chimeric antigen receptor (CAR) T cell therapies have revolutionized treatment of hematologic malignancies such as lymphoma and multiple myeloma. However, their success is limited by high manufacturing costs, reliance on autologous T cells, variable product quality, and life-threatening toxicities like cytokine release syndrome. In contrast, natural killer (NK) cells offer a safer, more flexible alternative, but their clinical translation remains constrained by complex expansion protocols and high production costs.

Here, we present a transformative approach using the human NK cell line YTS, which is amenable to large-scale culture, genetic manipulation, and cryopreservation. By introducing a CD19-specific CAR into YTS cells, we generate potent effector cells capable of selectively eliminating CD19-expressing targets. We demonstrate that CAR signaling in YTS cells requires intracellular activation and, in certain tumor settings, is enhanced by co-stimulation via the 2B4-CD48 pathway. Importantly, irradiation of YTS-CAR cells prevents proliferation without compromising their cytotoxic function even after freezing and thawing. In preclinical models, injections of irradiated YTS-CAR cells significantly reduced CD19+ tumor burden, underscoring their therapeutic promise.

This work positions engineered YTS cells as a novel, scalable, and cost-effective “off-the-shelf” immunotherapy platform suitable for treating refractory leukemias and lymphomas. Future studies will be required to assess safety and to explore applicability to autoimmune diseases and solid tumors.

Introduction

The expanding use of CAR-T cell therapy has revolutionized the treatment of lymphoma and myeloma.[1,2] Despite its success, this therapy still presents several limitations. A primary constraint involves the necessity for cell production from the patient due to the MHC restriction of T cells. This is a complex procedure that often uses T cells previously exposed to chemotherapy, affecting their quantity and functionality.[3,4] Additionally, CAR-T therapy can induce severe adverse effects, some of which may be life-threatening or irreversible, such as cytokine-release syndrome (CRS) and immune effector cell-associated neurotoxicity syndrome (ICANS).[5] Over the last few years, there has been growing interest in harnessing natural killer (NK) cells as an alternative platform.[6,7] NK cells are innate immune cells that play a pivotal role in eliminating virally-infected and cancer cells. One key advantage of NK cells over T cells is their lack of MHC restriction, allowing them to be used as off-the-shelf products. Furthermore, NK cells have shown no propensity to induce CRS or ICANS,[8] unlike CAR-T cells. NK cells can be obtained from various origins, primarily from peripheral and cord blood.[7] However, their production typically involves a complex and expensive process, potentially resulting in variations in the final product administered to patients. These complexities challenge the widespread clinical application of NK cells despite their advantages over T cells.

YTS is a subline of the NK cell line YT derived from a patient with acute lymphoblastic lymphoma.[9,10] YTS cells express $CD56^{dim}$ and have NK-like features,[9–11] most notably, cytotoxic activity *in vitro* and *in vivo.*[10] Unlike other NK cell products that express a combination of activating and inhibitory receptors, YTS cells lack inhibitory receptors[11] and appear to possess only two functional activating receptors: 2B4[12] and CD28.[13]

YTS cells present several compelling advantages over current NK cell-based immunotherapies. Unlike primary NK cells, which require donor-specific isolation and personalized

manufacturing processes that cause donor-to-donor variability, YTS cells grow robustly in culture, are inexpensive to maintain, and can be genetically manipulated with high efficiency. This makes them a stable, reproducible, and scalable cellular platform for immunotherapy. Their uniform phenotype and responsiveness eliminate the variability often seen with peripheral or cord blood–derived NK products.

In this study, we demonstrate that YTS cells engineered to express a CD19-specific CAR exhibit potent and selective cytotoxicity against CD19+ tumor cells both *in vitro* and *in vivo*. Moreover, we demonstrate that γ-irradiation inhibits YTS cell proliferation while maintaining their antitumor activity, an important step toward a safe, off-the-shelf NK cell therapy. Together, our findings position CAR-YTS cells as a promising and practical alternative to current NK or CAR-T therapies, with broad translational potential.

Methods

Cell lines

The cell lines used in this study included YTS-eco (abbreviated as YTS),[14] Raji, BJAB, MDA-MB-453, HEK293T, NK-92MI and the melanoma cell lines Mel526 and A375. All lines were cultured in-house, except the melanoma lines, kindly provided by Prof. Michal Lotem. NK-92MI cells were kindly provided by Dr. Aladin Samara and Dr. Galit Granot (Rabin Medical Center, Israel). Detailed culture conditions for each cell line are provided in the Supplementary Methods.

Cloning, generation of lentivirus particles and viral transduction

The coding sequences of human CD48 (NM_001778.4) and CD19 (NM_001178098.2) were cloned into the pHAGE-DsRED(−)-eGFP(+) lentiviral vector by Twist Bioscience. The CAR sequence targeting CD19 was derived from the FMC63-28Z construct (GenBank: HM852952.1). Two CAR constructs were expressed using lentiviral vectors: the first, obtained from Addgene (plasmid #135992), incorporated 4-1BB costimulatory signaling (FMC63-41BB-3z-P2A-EGFP); the second, based on HM852952.1, included CD28 signaling with an N-terminal FLAG tag in pHAGE-DsRED(−)-eGFP(+) lentiviral vector (Twist Bioscience). Experimental outcomes were consistent across both constructs, with no significant differences observed. For comparisons between YTS-CAR cells and other CAR-engineered cell therapies, the FLAG-CAR-CD28 construct was used in all cell types to ensure a uniform CAR design across platforms. Additionally, a truncated CAR variant was generated by retaining only two amino acids from the intracellular domain of CD28 (Twist Bioscience).[15]

Lentiviral virions were produced via transient three-plasmid transfection. HEK293T cells were co-transfected with the lentiviral vector containing the insert, a plasmid encoding PsPAx, and a plasmid encoding VSV-G, using TransIT-LT1 Transfection Reagent (Mirus Bio). Supernatants containing viral particles were collected 48 hours later and used to transduce the target cells.

Animal experiments

All animal experiments were conducted using female NOD scid gamma (NSG) mice, ages 8-12 weeks, bred and maintained in-house; Figure 5B was repeated once in male mice with similar results. Mice were housed under specific pathogen-free (SPF) conditions at the Hebrew University–Hadassah Medical School (Ein Kerem, Jerusalem). All procedures were approved by the Institutional Animal Care and Use Committee. Tumor size was measured regularly using calipers, and tumor volume was calculated using the formula: (length × width²) / 2.

Human samples

The study involving human samples was approved by the Institutional Helsinki Committee of Hadassah Medical Center. Peripheral blood samples were collected from CLL patients into heparinized tubes after obtaining written informed consent. PBMCs were isolated using a Ficoll gradient, and the mononuclear cell fraction was aliquoted and cryopreserved in freezing medium containing 90% fetal bovine serum (FBS) and 10% DMSO. Samples were thawed and used for experiments as needed.

Statistical analysis

Statistical analysis was performed using Microsoft Excel and GraphPad Prism software (version 7.02). Comparisons were made using Student's *t*-test or one-way ANOVA, as appropriate. A p-value < 0.05 was considered statistically significant.

Descriptions of the remaining methods are provided in Supplementary Data.

Results

YTS CAR CD19 efficiently kills CD19-positive targets

To utilize YTS cells therapeutically, we introduced a second-generation chimeric antigen receptor (CAR) against CD19 into these cells via lentiviral transduction. The CAR construct includes an anti-CD19 CAR linked to GFP via a P2A sequence and contains the 4-1BB and CD3ζ signaling domains. After sorting, we obtained a homogeneous population of GFP-positive cells (**Figure 1A**). We then performed an *in vitro* killing assay to evaluate CAR-CD19 function in YTS cells. Raji cells, which express CD19 (**Supplementary Figure 1),** were used as target cells and incubated with YTS-CAR CD19. The degree of target cell killing was quantified using Calcein-AM labeling. While Raji cells were only modestly killed by wild-type (WT) YTS cells, killing was significantly enhanced by YTS-CAR CD19 cells (**Figure 1B**). In

parallel, the CD19$^+$ B-cell line BJAB[16] was also efficiently and specifically killed by YTS-CAR CD19 cells (**Figure 1B**). Similar results were observed when chronic lymphocytic leukemia (CLL) cells, which also express CD19 (**Supplementary Figure 1**), were used as targets, as assessed by flow cytometry (**Figure 1C**).

Next, we aimed to verify that the enhanced killing observed in YTS-CAR CD19 cells was due to the activity of the introduced CAR and not merely improved engagement between YTS cells and the target cells. To achieve this, we expressed another CAR construct in YTS cells lacking the intracellular signaling domain, which has previously been shown to retain antigen-specific tumor-targeting capability[15] (see Methods). As before, we confirmed the transduction efficiency by examining GFP expression levels (**Figure 1D**). However, the truncated CAR construct did not demonstrate enhanced killing capability (**Figure 1E**). Therefore, we conclude that the intracellular signaling domain of the CAR is essential for its function in YTS cells.

We next evaluated degranulation and cytokine production by YTS-CAR CD19 cells. YTS-CAR CD19 cells exhibited relatively high baseline CD107a expression, consistent with the activated phenotype of this cell line. However, co-culture with Raji target cells resulted in a further increase in CD107a expression (**Supplementary Figure 2A**). In addition, YTS-CAR CD19 cells expressed high baseline levels of granzyme B, interferon-γ (IFN-γ), and tumor necrosis factor-α (TNF-α), with further increases in granzyme B and IFN-γ expression following co-culture with Raji cells (**Supplementary Figure 2B**). We also assessed the expression of inhibitory receptors to evaluate the exhaustion profile of YTS-CAR cells. While TIM-3 and LAG-3 were notably absent, PD-1 was expressed at baseline and further upregulated following co-culture with target cells (**Supplementary Figure 2C**). These findings indicate that, while YTS-CAR CD19 cells display basal activation, their effector function is further augmented upon target engagement.

We also investigated the potential of YTS cells to kill solid cancer cells. To test this, we expressed CD19 in the melanoma cell lines Mel526 and A375 (**Figure 2A,B**). YTS cells expressing the CAR against CD19 were able to specifically kill melanoma cells expressing CD19 (**Figure 2C,D**). In contrast, YTS cells expressing a truncated CAR lacking the intracellular signaling domain failed to mediate target cell killing, confirming that cytotoxicity depends on CAR signaling (**Figure 2C,D)**. This finding highlights the potential of YTS-CAR cells to recognize and kill non-hematologic cells when they express the relevant target antigen.

The 2B4-CD48 interaction is important for the killing of hematologic tumors by YTS CAR CD19

Previously, only two receptors, 2B4[12] and CD28,[13] were identified as active in YTS cells. However, the basal activity of YTS cells against target cells expressing the ligands for these receptors is low. Raji cells, which express CD48 (the ligand for 2B4) as well as CD80 and CD86 (the ligands for CD28) (**Supplementary Figure 1)**, were minimally killed by YTS cells (**Figure 1B**). Likewise, primary dendritic cells (DCs), which also express CD80 and CD86, were largely resistant to YTS-mediated killing (**Supplementary Figure 3**). Despite this, 2B4 and CD28 may still contribute to YTS-mediated cytotoxicity when YTS cells express CAR against CD19. To assess the importance of these receptors in CAR-CD19-mediated cytotoxicity, we generated MDA-MB-453 transfectants expressing CD19, CD48, or both (**Supplementary Figure 4**) and tested their susceptibility to YTS expressing CAR CD19 cells in a cytotoxicity assay (**Figure 3A)**. While the expression of CD19 or CD48 alone did not trigger significant killing, the co-expression of both ligands resulted in substantial cytotoxicity (**Figure 3A**). We also evaluated the expression of CD48, CD80, and CD86 in the melanoma cell lines Mel526 and A357. Despite these cell lines being efficiently killed by YTS cells expressing CAR CD19 (**Figure 2**), they exhibited low or minimal expression of these ligands (**Supplementary Figure 1**).

To further investigate the roles of these receptors, we either disrupted or blocked them in YTS cells. Using CRISPR, we knocked out 2B4 in YTS cells and subsequently overexpressed CAR targeting CD19 (**Figure 3B**). The deletion of 2B4 abolished the enhanced killing observed in CAR-expressing YTS cells when incubated with Raji cells (**Figure 3C**). To assess the role of CD28, we used a blocking antibody that has previously been shown to reduce YTS-mediated killing of 721.221 cells ([13] and **Supplementary Figure 5**). We applied this antibody in a cytotoxicity assay using YTS cells expressing CAR against CD19 and Raji cells, which express CD28 ligands (**Supplementary Figure 1**). However, blocking CD28 did not affect the killing of Raji cells by CAR-expressing YTS cells (**Figure 3D**). In conclusion, while CD28 does not appear to contribute to CAR-mediated killing by YTS cells, the 2B4-CD48 interaction may play a role in certain cell types, such as MDA-MB-453 and Raji. However, this interaction appears dispensable in melanoma cells, where robust cytotoxicity was observed despite the absence of the 2B4 ligand CD48 and the CD28 ligands CD80 and CD86.

Ensuring Safety and Efficacy: Irradiation of YTS-CAR Cells Retains Anti-Tumor Activity While Preventing Proliferation *in vitro* and *in vivo*

To use YTS cells therapeutically, they must be irradiated before injection into patients to prevent their proliferation. It is therefore essential to confirm that irradiation effectively prevents cell proliferation while preserving their cytotoxic activity. To evaluate the effects of irradiation on YTS cells *in vitro*, we employed several methods. First, we quantified the number of viable cells after exposing them to various irradiation doses. A minimum dose of 1000 rad effectively inhibited cell proliferation, as indicated by a reduction in viable cell numbers (**Figure 4A and Supplementary Figure 6A**). This observation was supported by an MTT assay, which demonstrated a decrease in metabolic activity beginning at doses as low as 1000 rad (**Figure 4B and Supplementary Figure 6B**). We also tested irradiated (2500 rad) YTS-

CAR cells following a freeze–thaw cycle and confirmed that they did not regain proliferative capacity (**Supplementary Figure 6C**).

To further assess proliferation, cells were labeled with a CellTrace dye, confirming that a 1000 rad dose was sufficient to prevent proliferation (**Figure 4C**). To investigate the *in vivo* impact of YTS cell irradiation, we subcutaneously injected NSG mice with CAR-CD19–expressing YTS cells exposed to varying radiation doses. Tumor growth was monitored over a follow-up period of 5 months. Mice receiving YTS cells that were non-irradiated or irradiated at 1000 rad developed tumors, whereas those injected with cells irradiated at 2000 rad or higher showed no tumor growth throughout a 5-month observation period (**Figure 4D**). Based on the results of both *in vitro* and *in vivo* experiments, we determined that a 2500 rad irradiation dose is effective in preventing cell proliferation. Next, we evaluated whether the cytotoxic activity of YTS cells expressing CAR was retained after irradiation at 2500 rad. Additionally, we froze the cells post-irradiation to simulate how these engineered YTS cells could be administered to patients. A cytotoxicity assay was performed, in which irradiated YTS cells, both with and without CAR targeting CD19, were incubated with Raji cells. The assay showed that YTS-CAR CD19 cells maintained their cytotoxic activity after irradiation and freezing (**Figure 4E**). Irradiated YTS-CAR cells retained cytotoxic activity for up to 6 days, with only a mild reduction over time (**Supplementary Figure 6D**). In addition, irradiated YTS-CAR cells were detectable in the circulation of mice for up to 24 hours after infusion (**Supplementary Figure 6E**). Since YTS cells harbor EBV consistent with latent infection[10,17], we further assessed whether EBV could be transferred to recipient cells. Co-culture experiments with HEK293T cells showed no evidence of EBV infection (**Supplementary Figure 6F**).

Comparison of YTS cells with other CAR-based cellular therapies and *in vivo* tumor control by irradiated YTS-CAR CD19 cells

We next compared the cytotoxic activity of YTS-CAR CD19 cells with other CAR-expressing cellular products. NK-92 is the most widely used NK cell line in clinical studies; however, these cells proliferate more slowly than YTS cells (**Supplementary Figure 7A**). To enable a direct comparison, YTS cells, NK-92 cells, and primary T cells were transduced with the same FLAG-tagged CAR construct containing a CD28 co-stimulatory domain (**Figure 5A, left, top**). Cytotoxicity assays were performed using equal numbers of Raji target cells and CAR-positive effector cells. To mimic clinical use, frozen-thawed effector cells were tested both before and after irradiation at the recommended dose for each cell type (CAR-T cells were not irradiated). YTS-CAR CD19 cells exhibited cytotoxic activity comparable to NK-92 CAR cells under both conditions and greater than that observed with primary CAR-T cells expressing the same construct (**Figure 5A, left**). We next compared cytokine secretion by the CAR-expressing NK cell lines following co-culture with target cells. YTS-CAR CD19 cells secreted higher levels of interferon-γ (IFN-γ) compared with NK-92 CAR cells after incubation with Raji cells (**Figure 5A, right**).

Finally, to assess the therapeutic function of YTS cells expressing CAR CD19 *in vivo*, we used a tumor model in which $7x10^6$ Raji cells were injected subcutaneously into NSG mice. Once tumors became palpable, we injected $20x10^6$ YTS CAR CD19 cells, which had been irradiated at 2500 rad and frozen, approximately twice a week for three weeks. As controls, we used non-transduced YTS cells or PBS. Tumor size was evaluated, and injection of YTS CAR CD19 cells resulted in a significant reduction in tumor size (~50%) (**Figure 5B, Supplementary Figure 7B**).

Discussion

Here, we demonstrate that genetically engineered YTS cells represent a promising approach to cellular therapy. As a proof of concept, we engineered YTS cells to express a CAR targeting

CD19, which showed enhanced activity both *in vitro* against CD19+ cell line and primary CLL cells, and *in vivo.*

NK cells offer several advantages over T cells for immunotherapy, including reduced adverse effects such as cytokine release syndrome and immune-effector cell-associated neurotoxicity.[6] Unlike T cells, NK cells are not restricted by major histocompatibility complex (MHC) compatibility, allowing their use a readily available off-the-shelf therapy. Additionally, NK cells exhibit natural cytotoxicity against tumor cells. Despite these advantages, NK cells face significant challenges as a therapeutic option. They represent a rare cell population, have a shorter lifespan than T cells *in vivo*, and are not easily manipulated. Various approaches have been developed to harness NK cells for immunotherapy. These include isolating primary NK cells from peripheral blood with modifications such as treatment with nicotinamide[18] or stimulation with IL-12, IL-15, and IL-18 to initiate a memory-like program.[19] Other sources include NK cells directly derived from cord blood,[8,20] those matured from cord blood stem cells,[21] or NK cells derived from human induced pluripotent stem cells (iPSCs).[22] Another notable source of NK cells is the NK-92 cell line, which has been investigated as a therapeutic option for various tumors with modifications such as the expression of different chimeric antigen receptors (CARs).[23] NK-92-based CAR therapies have been evaluated in several clinical trials, including CARs targeting HER2[24] and CD33.[25] However, despite their therapeutic potential, NK-92 cells present practical limitations: they proliferate relatively slowly (**Supplementary Figure 7A**), require specialized culture conditions,[26] and can be challenging to genetically modify (personal observation), all of which may complicate clinical translation. In addition, the broader receptor repertoire of NK-92 cells compared to YTS cells[27] may increase the risk of off-target effects. In our study, YTS-CAR CD19 cells demonstrated cytotoxic activity comparable to NK-92 cells expressing the same CAR construct, while exhibiting higher secretion of interferon-γ (IFN-γ). Increased IFN-γ production has been

associated with improved anti-tumor responses, including in CAR-T cell therapies,[28,29] and especially in the case of solid cancers.[30]

YTS cells offer several advantages over other NK cell sources. They are easy to culture, readily transfected to express additional receptors, and naturally lack inhibitory receptors. Unlike most NK cells, which rely on a delicate balance of complex activating and inhibitory receptors,[31] YTS cells have only a few active receptors.[12,13] This limited receptor repertoire minimizes off-target effects while allowing for precise targeting of antigens. Additionally, unlike CAR-T cells, YTS cells do not require specialized collection processes and can be administered immediately to patients, eliminating production delays. We did not directly assess the potential of YTS cells to induce CRS,[32] as this is not reliably modeled in NSG mice. However, clinically significant CRS or neurotoxicity has not been observed in studies using other NK cell-based platforms.[8,33] These features make YTS cells an accessible and potent NK cell source, addressing key limitations of CAR-T therapies, particularly technical challenges and high costs.[34–36] To address safety, we performed a series of *in vitro* and *in vivo* experiments to determine the irradiation dose required to prevent cellular proliferation. Irradiation at ≥2000 rad resulted in irreversible loss of proliferative capacity and progressive cell death. *In vivo*, irradiated YTS-CAR cells were injected into immunodeficient mice and monitored for up to 5 months, with no evidence of tumor formation. Although irradiated cells did not exhibit proliferative capacity *in vitro* or *in vivo*, additional analyses of genomic instability or transformation markers could provide further safety information and should be evaluated in future studies. In addition, YTS cells, as a subclone of the YT NK-like lymphoma line, harbor Epstein–Barr virus (EBV) consistent with latent infection.[10,17] The theoretical risk associated with EBV carriage is mitigated by pre-infusion irradiation, which abolishes proliferative capacity, as well as by the intended short-lived, non-engrafting use of these cells, as confirmed by our *in vitro* experiments. Notably, the NK-92 cell line has also been reported to contain

EBV DNA sequences,[37–39] and irradiated NK-92 cells have been administered clinically without evidence of EBV-related safety concerns. In terms of treatment efficacy, although we observed an approximately 50% reduction in tumor size, our model does not fully recapitulate lymphoma, as tumor cells were implanted subcutaneously. Importantly, YTS cells also secrete high levels of IFN-γ, a potent immunomodulator whose full therapeutic potential is likely underestimated in this immunodeficient mouse model. While only a single $CD19^+$ tumor model was evaluated *in vivo*, additional $CD19^+$ target cells were shown to be susceptible to YTS-CAR-mediated killing *in vitro*, supporting the broader cytotoxic potential of these cells. Finally, we have not compared YTS-CAR to CAR-T *in vivo*, as both platforms have fundamentally different kinetics, which would make a direct comparison difficult to interpret.

Mechanistically, we demonstrate that CAR activity against CD19 relies on intracellular signaling, indicating that its effectiveness is not solely due to CAR-target cell engagement. Additionally, we show that for some tumors the CAR's function depends on the 2B4-CD48 axis, suggesting that this pathway should be evaluated in specific tumor types. It remains unclear why melanoma cells, which were resistant to YTS-mediated killing at baseline, became susceptible to YTS-CAR-mediated cytotoxicity upon CD19 expression, unlike MDA cells. This differential response may be due to the expression of a co-stimulatory ligand by melanoma cells that engages a receptor on YTS cells, providing a secondary activation signal effective only with CAR engagement.

We assessed the effect of CD19-targeted CARs in YTS cells, as this is the most widely studied CAR. However, it is plausible that other CARs may also be effective in YTS cells. Moreover, additional elements can be transduced into YTS cells, positioning them as a versatile platform for diverse receptor expression and expanded therapeutic potential. However, although the irradiated NK-92 cell line has been used in clinical trials, demonstrating the safety of this approach, the safety of irradiated YTS cells will need to be carefully evaluated in future studies.

References

1. Grégoire C, Coutinho de Oliveira B, Caimi PF, Caers J, Melenhorst JJ. Chimeric antigen receptor T-cell therapy for haematological malignancies: Insights from fundamental and translational research to bedside practice. Br J Haematol. 2024;205(5):1699-1713.

2. Brudno JN, Kochenderfer JN. Chimeric antigen receptor T-cell therapies for lymphoma. Nat Rev Clin Oncol. 2018;15(1):31-46.

3. Das RK, O'Connor RS, Grupp SA, Barrett DM. Lingering effects of chemotherapy on mature T cells impair proliferation. Blood Adv. 2020;4(19):4653-4664.

4. Herzberg C, Schiele P, Walter AL, et al. Prior chemotherapy deteriorates T-cell quality for CAR T-cell therapy in B-cell non-Hodgkin's lymphoma. J Immunother Cancer. 2025;13(4):e010709.

5. Morris EC, Neelapu SS, Giavridis T, Sadelain M. Cytokine release syndrome and associated neurotoxicity in cancer immunotherapy. Nat Rev Immunol. 2022;22(2):85-96.

6. Berrien-Elliott MM, Jacobs MT, Fehniger TA. Allogeneic natural killer cell therapy. Blood. 2023;141(8):856-868.

7. Laskowski TJ, Biederstädt A, Rezvani K. Natural killer cells in antitumour adoptive cell immunotherapy. Nat Rev Cancer. 2022;22(10):557-575.

8. Liu E, Marin D, Banerjee P, et al. Use of CAR-Transduced natural killer cells in CD19-positive lymphoid tumors. N Engl J Med. 2020;382(6):545-553.

9. Yodoi J, Teshigawara K, Nikaido T, et al. TCGF (IL 2)-receptor inducing factor(s). I. Regulation of IL 2 receptor on a natural killer-like cell line (YT cells). J Immunol. 1985;134(3):1623-1630.

10. Yoneda N, Tatsumi E, Kawano S, et al. Detection of Epstein-Barr virus genome in natural-killer-like cell line, YT. Leukemia. 1992;6(2):136-141.

11. Gunesch JT, Angelo LS, Mahapatra S, et al. Genome-wide analyses and functional profiling of human NK cell lines. Mol Immunol. 2019;115:64-75.

12. Elias S, Yamin R, Golomb L, et al. Immune evasion by oncogenic proteins of acute myeloid leukemia. Blood. 2014;123(10):1535-1543.

13. Chen X, Allan DSJ, Krzewski K, Ge B, Kopcow H, Strominger JL. CD28-stimulated ERK2 phosphorylation is required for polarization of the microtubule organizing center and granules in YTS NK cells. Proc Natl Acad Sci U S A. 2006;103(27):10346-10351.

14. Baba E, Erskine R, Boyson JE, et al. N-linked carbohydrate on human leukocyte antigen-C and recognition by natural killer cell inhibitory receptors. Hum Immunol. 2000;61(12):1202-1218.

15. Fleischer LC, Becker SA, Ryan RE, Fedanov A, Doering CB, Spencer HT. Non-signaling Chimeric Antigen Receptors Enhance Antigen-Directed Killing by γδ T Cells in Contrast to αβ T Cells. Mol Ther Oncolytics. 2020;18:149-160.

16. Fujita N, Jaye DL, Geigerman C, et al. MTA3 and the Mi-2/NuRD complex regulate cell fate during B lymphocyte differentiation. Cell. 2004;119(1):75-86.

17. Kanegane H, Wang F, Tosato G. Virus-cell interactions in a natural killer-like cell line from a patient with lymphoblastic lymphoma. Blood. 1996;88(12):4667-4675.

18. Cichocki F, Zhang B, Wu C-Y, et al. Nicotinamide enhances natural killer cell function and yields remissions in patients with non-Hodgkin lymphoma. Sci Transl Med. 2023;15(705):eade3341.

19. Berrien-Elliott MM, Cashen AF, Cubitt CC, et al. Multidimensional analyses of donor memory-like NK cells reveal new associations with response after adoptive immunotherapy for leukemia. Cancer Discov. 2020;10(12):1854-1871.

20. Marin D, Li Y, Basar R, et al. Safety, efficacy and determinants of response of allogeneic CD19-specific CAR-NK cells in CD19+ B cell tumors: a phase 1/2 trial. Nat Med. 2024;30(3):772–784.

21. Domogala A, Blundell M, Thrasher A, Lowdell MW, Madrigal JA, Saudemont A. Natural killer cells differentiated in vitro from cord blood CD34+ cells are more advantageous for use as an immunotherapy than peripheral blood and cord blood natural killer cells. Cytotherapy 2017;19(6):710-720.

22. Li Y, Hermanson DL, Moriarity BS, Kaufman DS. Human iPSC-derived natural killer cells engineered with chimeric antigen receptors enhance anti-tumor activity. Cell Stem Cell. 2018;23(2):181-192.e5.

23. Suck G, Odendahl M, Nowakowska P, et al. NK-92: an "off-the-shelf therapeutic" for adoptive natural killer cell-based cancer immunotherapy. Cancer Immunol Immunother. 2016;65(4):485-492.

24. Burger MC, Forster M-T, Romanski A, et al. Intracranial injection of natural killer cells engineered with a HER2-targeted chimeric antigen receptor in patients with recurrent glioblastoma. Neuro Oncol. 2023;25(11):2058-2071.

25. Tang X, Yang L, Li Z, et al. First-in-man clinical trial of CAR NK-92 cells: safety test of CD33-CAR NK-92 cells in patients with relapsed and refractory acute myeloid leukemia. Am J Cancer Res. 2018;8(6):1083-1089.

26. Klingemann H. The NK-92 cell line-30 years later: its impact on natural killer cell research and treatment of cancer. Cytotherapy. 2023;25(5):451-457.

27. Jarahian M, Fiedler M, Cohnen A, et al. Modulation of NKp30- and NKp46-mediated natural killer cell responses by poxviral hemagglutinin. PLoS Pathog. 2011;7(8):e1002195.

28. Sánchez-Paulete AR, Mateus-Tique J, Mollaoglu G, et al. Targeting macrophages with CAR T cells delays solid tumor progression and enhances antitumor immunity. Cancer Immunol Res. 2022;10(11):1354-1369.

29. Mateus-Tique J, Lakshmi A, Singh B, et al. Armored macrophage-targeted CAR-T cells reset and reprogram the tumor microenvironment and control metastatic cancer growth. Cancer Cell. 2026;44(3):534-550.e11.

30. Larson RC, Kann MC, Bailey SR, et al. CAR T cell killing requires the IFNγR pathway in solid but not liquid tumours. Nature. 2022;604(7906):563-570.

31. Quatrini L, Della Chiesa M, Sivori S, Mingari MC, Pende D, Moretta L. Human NK cells, their receptors and function. Eur J Immunol. 2021;51(7):1566-1579.

32. Duncan BB, Dunbar CE, Ishii K. Applying a clinical lens to animal models of CAR-T cell therapies. Mol Ther Methods Clin Dev. 2022;27:17-31.

33. Ghobadi A, Bachanova V, Patel K, et al. Induced pluripotent stem-cell-derived CD19-directed chimeric antigen receptor natural killer cells in B-cell lymphoma: a phase 1, first-in-human trial. Lancet. 2025;405(10473):127-136.

34. Battiwalla M, Tees M, Flinn I, et al. Access barriers to anti-CD19+ CART therapy for NHL across a community transplant and cellular therapy network. Blood Adv. 2025;9(2):429-435.

35. Gajra A, Zalenski A, Sannareddy A, Jeune-Smith Y, Kapinos K, Kansagra A. Barriers to chimeric antigen receptor T-Cell (CAR-T) therapies in clinical practice. Pharmaceut Med. 2022;36(3):163-171.

36. Haslam A, Hoeg TB, Prasad V. Estimation of eligibility for and response to CAR-T therapy in the United States. Blood Adv. 2024;8(4):1032-1036.

37. Cellosaurus cell line NK-92 (CVCL_2142). https://www.cellosaurus.org/CVCL_2142 Accessed on February 19, 2026.

38. German Collection of Microorganisms and Cell Cultures GmbH: Welcome to the Leibniz Institute DSMZ | NK-92. https://www.webshop.dsmz.de/en/human-animal-cell-lines/NK-92.html Accessed on February 19, 2026.

39. NK-92® - CRL-2407 | ATCC. https://www.atcc.org/products/crl-2407 Accessed on February 19, 2026.

Figures legends

Figure 1. YTS expressing CAR against CD19. A) FACS verification of CAR CD19 expression in YTS cells; (B, C) Killing experiments: tumor cells (Raji and BJAB, B or primary CLL cells, C) were incubated with YTS cells expressing CAR against CD19 or an empty vector. For B, E:T 20:1, repeated four times; For C, E:T 20:1, repeated in two different patients. D) FACS verification of CAR CD19 with truncated intra-cellular domain expressed in YTS cells. E) Killing experiment: YTS cells expressing CAR CD19, truncated CAR CD19 or an empty vector, were incubated with Raji cells, E:T 20:1, repeated two times. Killing experiments were performed in at least five technical repeats and target cells were labeled with Calcein AM. ***, P<0.001, ****, P<0.0001, Student's *t*-test. CLL – chronic lymphocytic leukemia, E:T – Effector: Target.

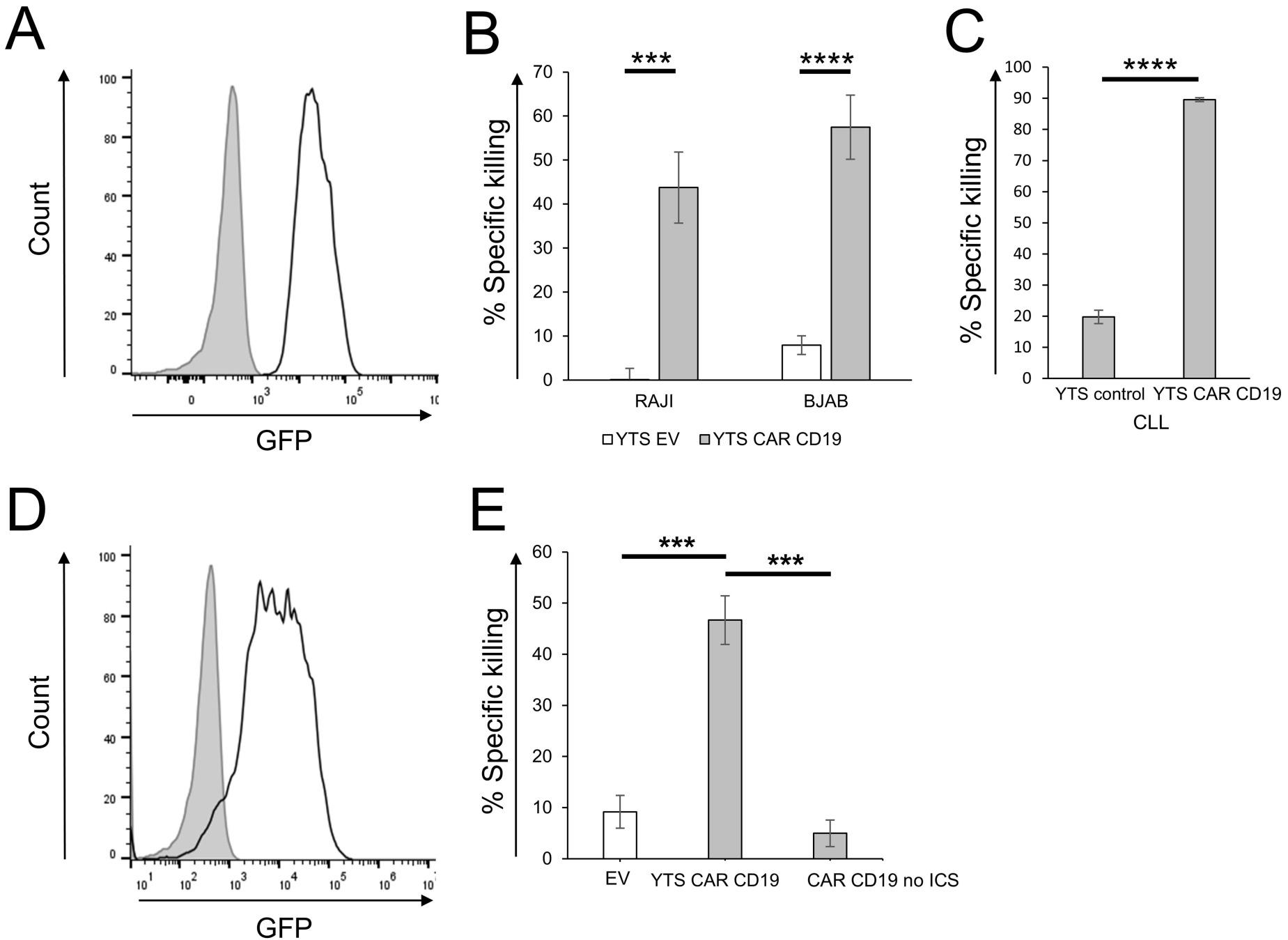
Figure 2. Activity of YTS cells against melanoma cell lines. (A, B) Expression of CD19 in melanoma cell lines: Mel526 (left) and A357 (right). Cells were stained by FACS for CD19. (C, D) Killing assays: melanoma cell lines (Mel526, C; A357, D) with and without CD19 expression were labeled with Calcein AM and then incubated with YTS cells expressing CAR against CD19, a truncated CAR lacking the intracellular signaling domain, or an empty vector. E:T 20:1. One experiment is presented out of two performed, the killing experiments were performed in six replicates. ***, P<0.001, Student's *t*-test or ANNOVA with multiple comparisons.

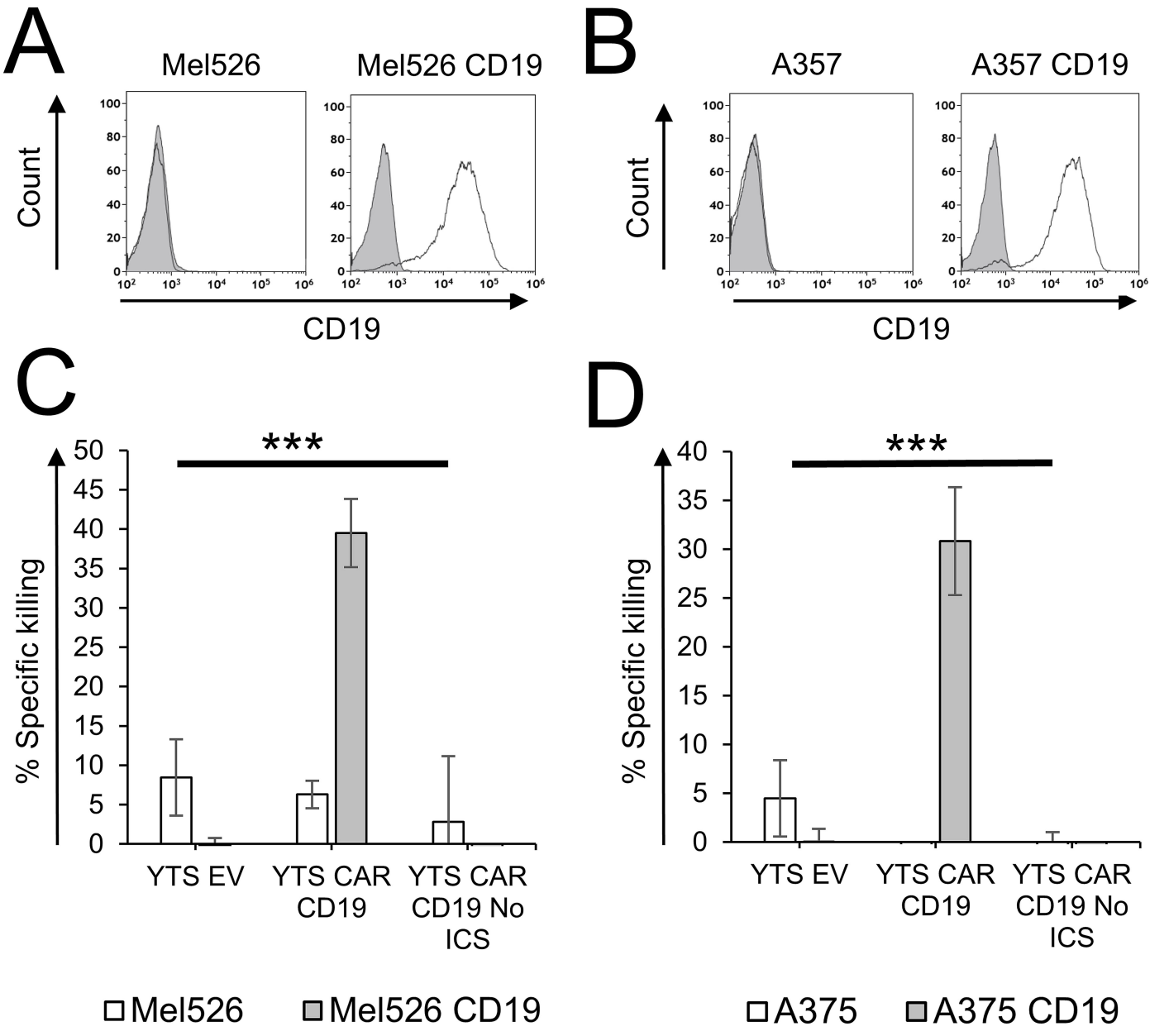
Figure 3. Interaction of CAR against CD19 with other receptors in YTS cells. (A) Killing assays with MDA-MB-453 transfectants expressing empty vector, CD19, CD48 or both CD19 and CD48 were incubated with YTS WT or YTS expressing CAR against CD19. (B, C) FACS analysis showing 2B4 expression (left) and GFP expression (right), where GFP serves as a reporter for CAR expression, in YTS cells with 2B4 KO expressing CAR against CD19. (C) Killing assay: YTS expressing CAR against CD19 or YTS expressing CAR against CD19 with 2B4 KO were incubated with Raji cells, E:T 20:1. (D) Killing assay: YTS cells expressing CAR against CD19 were pre-incubated with either a control antibody or an anti-CD28 antibody before being incubated with target cells at an E:T ratio of 20:1. All experiments were performed at least twice, killing experiments were performed in six replicates and target cells were labeled with Calcein AM, ***, $P<0.001$, Student's *t*-test.

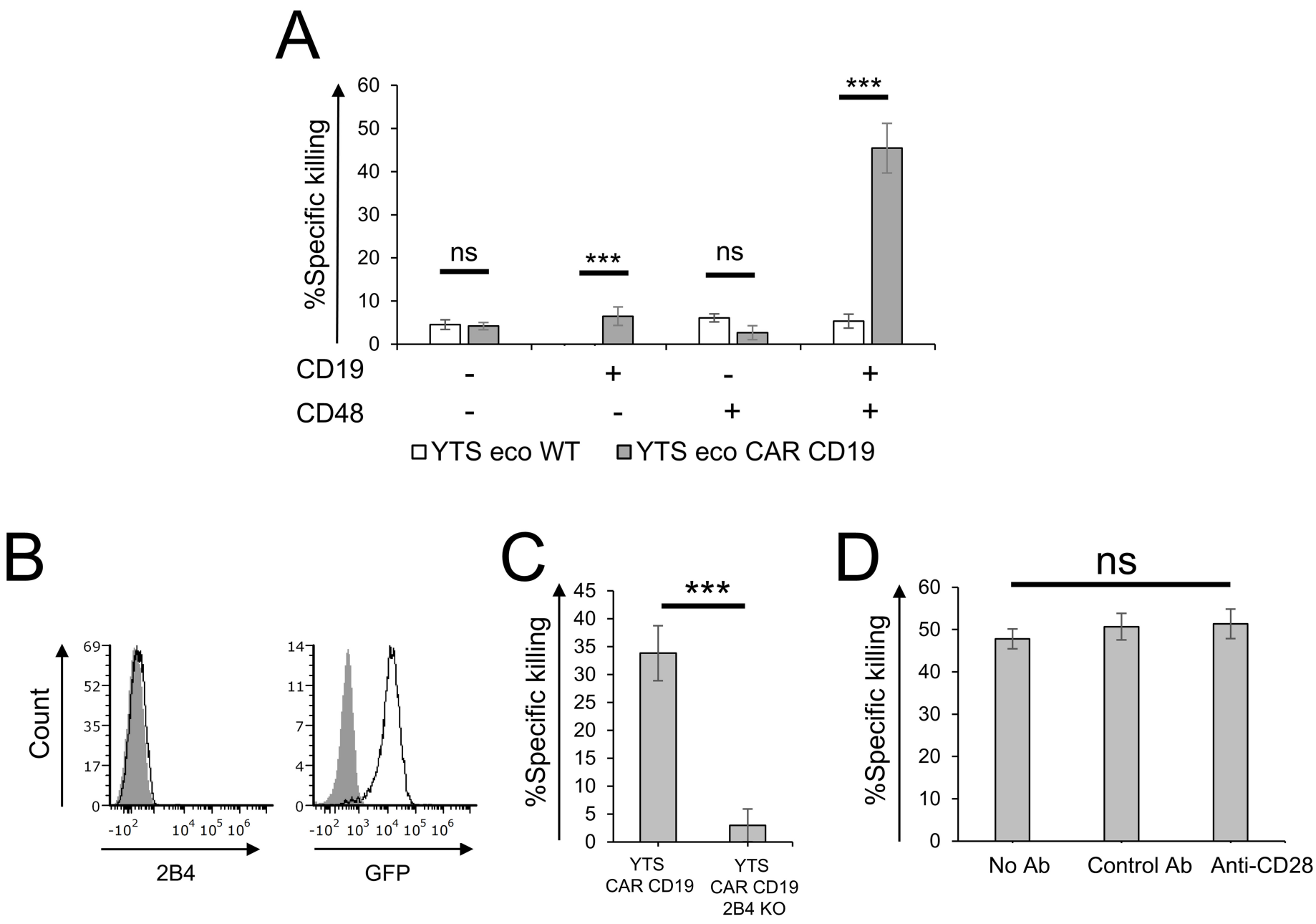
Figure 4. Safety and efficiency of irradiated YTS cells. A-C) YTS cells expressing CAR against CD19 were non-irradiated or irradiated at different levels and then subjected for various viability and proliferation tests along different time points (repeated in two independent experiments): (A) Viability test, where the number of viable cells was detected by FACS; (B) MTT assay to assess the metabolic activity of the cells, and (C) Proliferation assay to test the proliferation capacity of the cells using CellTrace. (D) $7x10^6$ YTS CAR CD19 cells were irradiated at various doses and subsequently injected subcutaneously into NSG mice. Tumor development was monitored over time. Each group included four mice. The results were repeated in another independent experiment. (E) YTS cells expressing either a CAR against CD19 or an empty vector were irradiated with 2500 rad or left non-irradiated, then frozen and later used in a killing assay against Raji cells. The degree of killing was assessed by FACS at multiple time points over 48 hours. Representative raw flow cytometry plots of Raji cells after

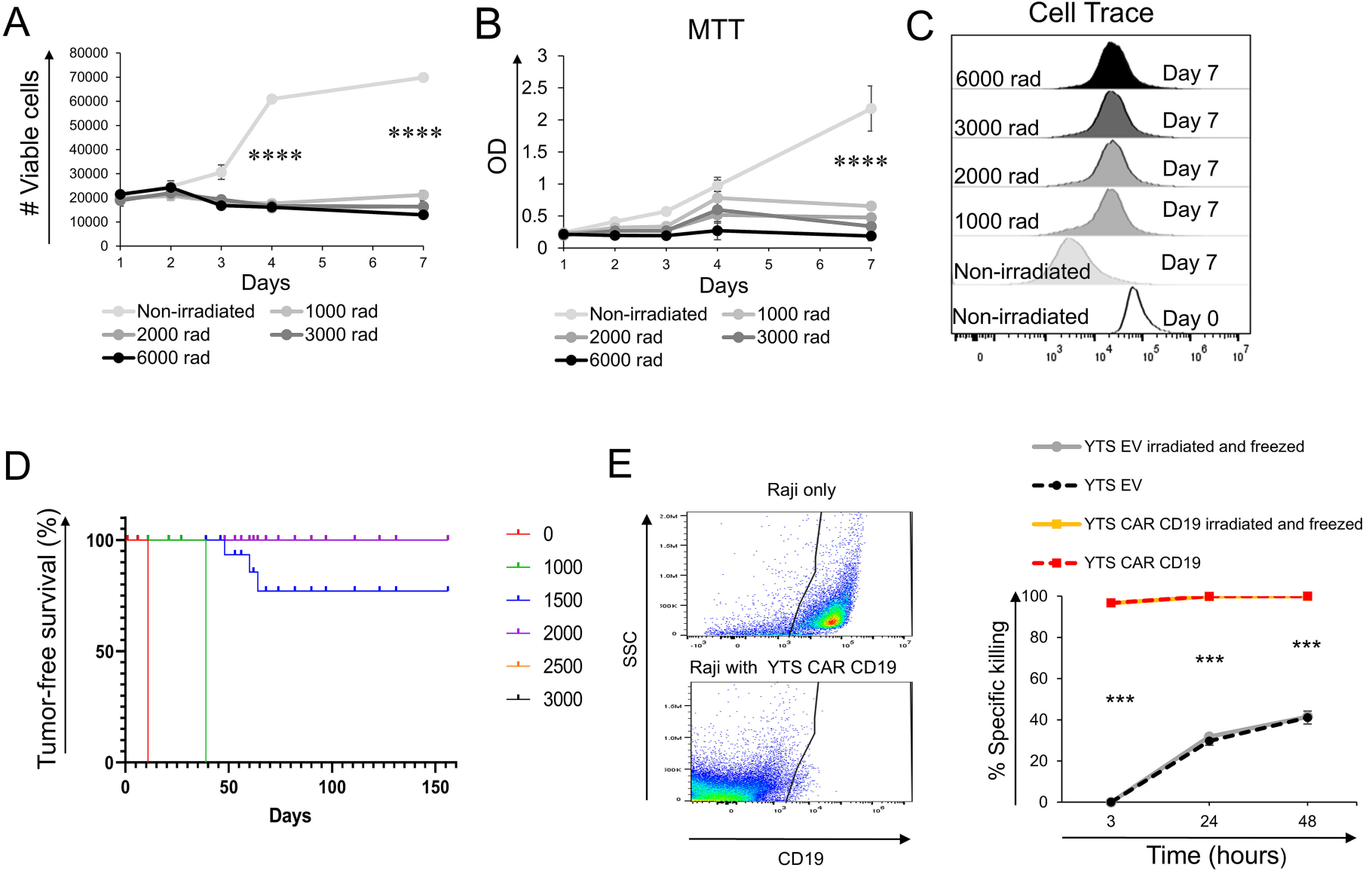
24 hours are shown on the left. E:T 20:1. ***, P<0.001, ANOVA test with multiple comparisons (A, B, E).

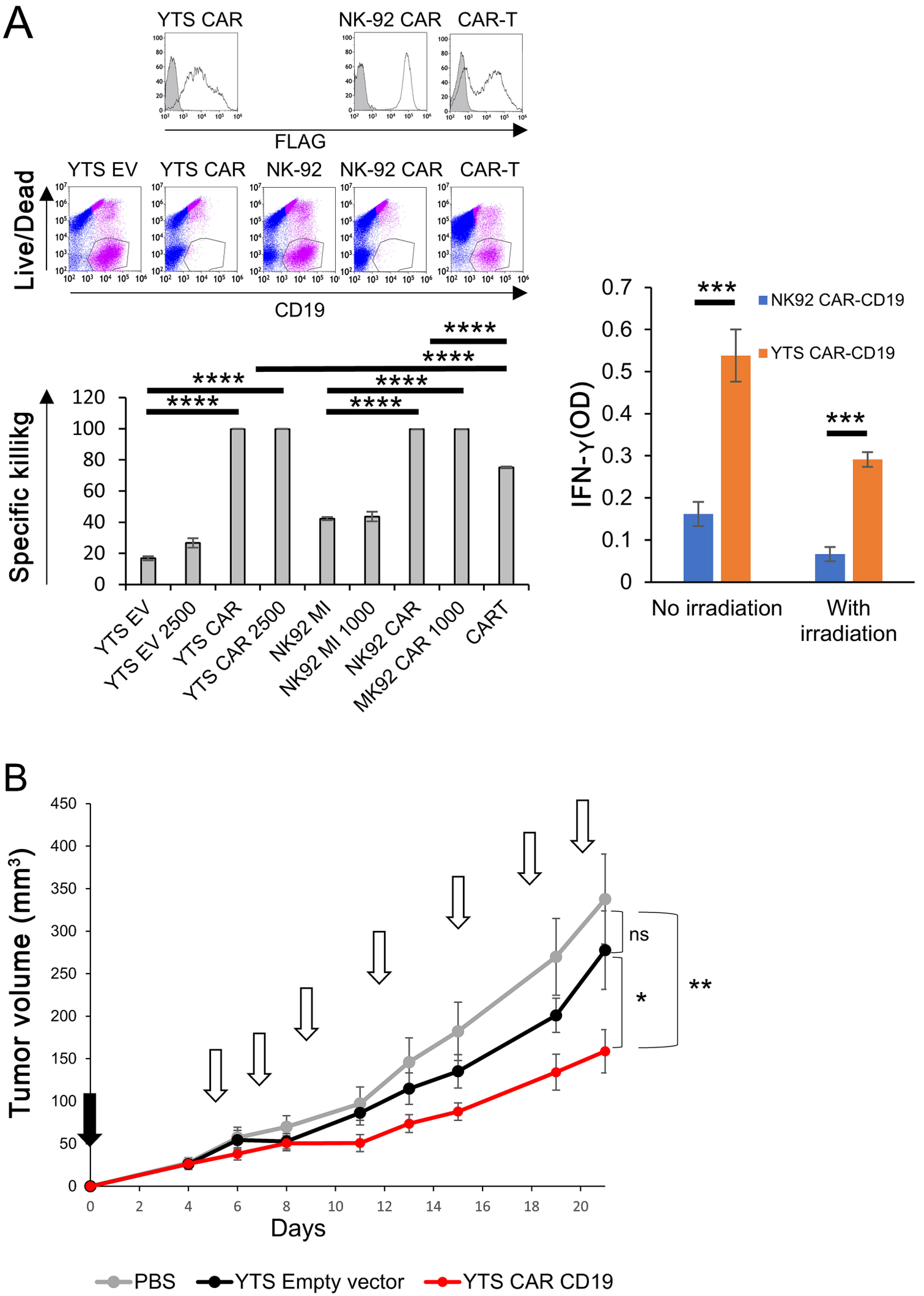
Figure 5. Comparison of YTS-CAR CD19 cells with other CAR-based effectors and *in vivo* activity of YTS-CAR CD19. (A) Left: YTS cells, NK-92MI cells or primary T cells expressing a CD19-targeted CAR (YTS-CAR, NK-92 CAR, and CAR-T, respectively) were co-cultured with Raji target cells at an effector-to-target (E:T) ratio of 10:1. All CAR constructs were identical and included a FLAG tag to enable detection of CAR expression. Frozen-thawed effector cells were either left untreated or irradiated prior to the assay (YTS: 2500 rad; NK-92: 1000 rad). CAR-T cells were not irradiated. For CAR-expressing cells, input cell numbers was adjusted to ensure equivalent numbers of CAR-positive cells across conditions, based on FLAG expression (shown above). Cytotoxicity was assessed by flow cytometry after 3 hours of incubation. Data shown are representative of two independent experiments with similar results. Right: IFN-γ secretion by YTS-CAR and NK-92 CAR CD19 cells following co-culture with Raji target cells at an E:T ratio of 5:1 for 24 hours. Supernatants were collected and analyzed by ELISA. (B) *In vivo* assessment of YTS-CAR CD19 cells in tumor-bearing immunodeficient mice. $7x10^6$ Raji cells were injected subcutaneously into immunodeficient mice (indicated by a filled arrow). Once tumors became palpable, mice were treated with $20x10^6$ YTS cells expressing CAR-CD19, untransduced YTS cells, or PBS, injected twice weekly (indicated by hollow arrows). YTS cells were irradiated at 2500 rad and cryopreserved prior to injection. Tumor volumes were monitored throughout the experiment. Similar results were observed in two additional independent experiments (one using cells irradiated at 1000 rad and another using cells irradiated at 2500 rad administered approximately three times per week). * P<0.05, ** P<0.01, **** P<0.0001, ANOVA with multiple comparisons (A), Student's *t*-test (B).


A
Count
GFP
B
% Specific killing
***
****
RAJI
BJAB
YTS EV
YTS CAR CD19
C
% Specific killing
****
YTS control
YTS CAR CD19
CLL
D
Count
GFP
E
% Specific killing
***
***
EV
YTS CAR CD19
CAR CD19 no ICS


A
Mel526
Mel526 CD19
Count
CD19
B
A357
A357 CD19
Count
CD19
C
***
% Specific killing
YTS EV
YTS CAR CD19
YTS CAR CD19 No ICS
Mel526
Mel526 CD19
D
***
% Specific killing
YTS EV
YTS CAR CD19
YTS CAR CD19 No ICS
A375
A375 CD19


A
%Specific killing
60
50
40
30
20
10
0
ns
***
ns
***
CD19
-
+
-
+
CD48
-
-
+
+
YTS eco WT
YTS eco CAR CD19
B
Count
69
52
35
17
0
-10^2
10^4 10^5 10^6
2B4
14
11
7
4
0
-10^2 10^3 10^4 10^5 10^6
GFP
C
%Specific killing
45
40
35
30
25
20
15
10
5
0
***
YTS CAR CD19
YTS CAR CD19 2B4 KO
D
%Specific killing
60
50
40
30
20
10
0
ns
No Ab
Control Ab
Anti-CD28


A
Viable cells
80000
70000
60000
50000
40000
30000
20000
10000
0
1
2
3
4
5
6
7
Days
****
****
Non-irradiated
1000 rad
2000 rad
3000 rad
6000 rad
B
MTT
OD
3
2.5
2
1.5
1
0.5
0
Days
****
Non-irradiated
1000 rad
2000 rad
3000 rad
6000 rad
C
Cell Trace
6000 rad
Day 7
3000 rad
Day 7
2000 rad
Day 7
1000 rad
Day 7
Non-irradiated
Day 7
Non-irradiated
Day 0
D
Tumor-free survival (%)
100
50
0
0
50
100
150
Days
0
1000
1500
2000
2500
3000
E
Raji only
Raji with YTS CAR CD19
SSC
CD19
YTS EV irradiated and freezed
YTS EV
YTS CAR CD19 irradiated and freezed
YTS CAR CD19
% Specific killing
100
80
60
40
20
0
***
***
***
3
24
48
Time (hours)


A
YTS CAR
NK-92 CAR
CAR-T
FLAG
YTS EV
YTS CAR
NK-92
NK-92 CAR
CAR-T
Live/Dead
CD19
Specific killikg
****
****
****
****
****
YTS EV
YTS EV 2500
YTS CAR
YTS CAR 2500
NK92 MI
NK92 MI 1000
NK92 CAR
MK92 CAR 1000
CART
IFN-γ(OD)
***
***
NK92 CAR-CD19
YTS CAR-CD19
No irradiation
With irradiation
B
Tumor volume (mm³)
Days
ns
*
**
PBS
YTS Empty vector
YTS CAR CD19

Supplementary Methods

Cell lines

Raji and YTS cells were cultured in RPMI-1640 medium (Sigma-Aldrich), while MDA-MB-453 and HEK293T cells were maintained in Dulbecco's Modified Eagle Medium (DMEM, Sigma-Aldrich). Culture media were supplemented with 10% heat-inactivated fetal bovine serum (FBS, Sigma-Aldrich), 1 mM sodium pyruvate (Biological Industries), 2 mM glutamine (Biological Industries), non-essential amino acids (Biological Industries), 100 U/mL penicillin (Biological Industries), and 0.1 mg/mL streptomycin (Biological Industries). All cells were maintained at 37°C in a humidified incubator with 5% CO_2. The melanoma cell lines Mel526 and A375 were cultured in a mixed medium comprising 75% DMEM, 25% RPMI-1640, and 8.75% Ham's F-12 (Biowest), supplemented with 10% heat-inactivated FBS, 1.25% HEPES buffer (Biological Industries), 1.25% 100 mM glutamine, and 1.25% penicillin-streptomycin. NK-92MI cells were maintained in α-MEM without ribonucleosides (low glucose) (Sartorius) supplemented with 12.5% heat-inactivated FBS, 12.5% heat-inactivated horse serum (Merck), 2 mM L-glutamine, 1 mM sodium pyruvate, 1× non-essential amino acids, and penicillin (100 U/mL)–streptomycin (0.1 mg/mL). The medium was further supplemented with 0.2 mM myo-inositol (Merck), 0.1 mM 2-mercaptoethanol (Merck), and 0.02 mM folic acid (Merck).

Antibodies

Antibodies used for FACS analysis included: APC anti-human CD19 (BioLegend; cat. no. 302212), APC anti-human CD48 (BioLegend; cat. no. 336714), APC anti-human CD244 (2B4) (BioLegend; cat. no. 329512), APC anti-human CD80 (BioLegend; cat. no. 305220), APC anti-human CD86 (BioLegend; cat. no. 374208), PE anti-human CD352 (NTB-A) (BioLegend; cat. no. 317208), Anti-Human CD28 (BD; cat. no. BD348040).

Isotype control antibodies used: APC Mouse IgG1, κ (BioLegend; cat No. 400120) and PE Mouse IgG1, κ (BioLegend; cat no. 400112).

FACS staining

For FACS staining, cells were counted and plated in 96-well U-bottom plates at a density of 100,000 cells per well. Cells were incubated with antibodies under the following conditions: Unconjugated primary antibodies were added at 0.2 μg per well and incubated on ice for 1 hour. After incubation, cells were centrifuged at 1600 rpm for 5 minutes at 4°C, and a fluorophore-conjugated secondary anti-mouse antibody was added at a 1:200 dilution. For directly conjugated antibodies, staining was performed using a 1:200 dilution with a 30-minute incubation on ice. Following staining, cells were either analyzed immediately or fixed with 1% paraformaldehyde (PFA) for later acquisition. FACS analysis was performed using a DxFLEX or CytoFLEX flow cytometer.

Lentivirus production

Lentiviral virions were produced via transient three-plasmid transfection. HEK293T cells were co-transfected with the lentiviral transfer vector encoding the CAR construct, a packaging plasmid (psPAX2), and a plasmid encoding VSV-G, using TransIT-LT1 Transfection Reagent (Mirus Bio) according to the manufacturer's instructions. Supernatants containing viral particles were collected 48 hours post-transfection, filtered through a 0.45 μm filter, and used immediately or stored at −70°C until use.

Intracellular cytokine and cytotoxic molecule staining

For assessment of cytokine production and cytotoxic effector molecules, YTS-CAR cells (2×10^6) were co-cultured with Raji target cells (1×10^5) at a 20:1 effector-to-target (E:T) ratio in RPMI complete medium (500 μL + 500 μL). Control wells contained YTS-CAR cells alone.

Cells were incubated for 3 hours at 37°C in the presence of GolgiPlug (1:1000; BD Biosciences, cat. no. 554714).

Following incubation, 200 µL of cells were collected, washed with FACS buffer, and stained for surface CD56-PE (BioLegend, cat. no. 318306; 1:200 dilution) for 30 minutes on ice. Cells were then fixed and permeabilized using BD Cytofix/Cytoperm solution (cat. no. BD554714, BD Biosciences) for 30 minutes at room temperature. After washing with Perm/Wash buffer, intracellular staining was performed using antibodies against granzyme B-APC (BioLegend, cat. no. 396408), IFN-γ-BV650 (BioLegend, cat. no. 502538), and TNF-α-BV785 (BioLegend, cat. no. 502948), each diluted 1:100 in Perm/Wash buffer. Cells were washed and analyzed by a DxFLEX flow cytometer (Beckman Coulter).

Exhaustion marker analysis

To evaluate expression of exhaustion markers, YTS-CAR cells (2×10^6) were co-cultured with Raji cells (1×10^5) at a 20:1 E:T ratio in RPMI complete medium for 24 hours at 37°C. Following incubation, 200 µL of cells were collected, washed, and stained with the following antibodies diluted 1:100 in FACS buffer for 30 minutes on ice: TIM-3-PE (Thermo Fisher, cat. no. 12-3109-42), PD-1-PC5.5 (Beckman Coulter, cat. no. B36123), and LAG-3-AF647 (Thermo Fisher, cat. no. 51-2239-42). Cells were washed and analyzed by flow cytometry using a DxFLEX instrument.

CD107a degranulation assay

Degranulation was assessed by measuring surface CD107a expression. YTS-CAR cells (1×10^5) were co-cultured with Raji target cells (1×10^5) at a 1:1 ratio in 200 µL RPMI complete medium. Anti-CD107a-APC (BioLegend, cat. no. 328620) and CD56-PE (BioLegend, cat. no. 318306) were added at the beginning of the incubation (0.2 µg per well). Cells were incubated for 2 hours at 37°C, washed with FACS buffer, and analyzed by flow cytometry on a DxFLEX instrument.

Viral transduction

For transduction, YTS and NK-92MI cells were resuspended in viral supernatant and seeded in 96-well U-bottom plates, followed by spinoculation at 1800 rpm for 90 minutes at 32°C. Cells were then incubated overnight at 37°C and cultured under standard conditions. CAR-expressing cells were purified by FACS (SH800, Sony) based on GFP or FLAG expression. The gating strategy included exclusion of debris based on forward and side scatter, and selection of GFP^+ or $FLAG^+$ live cells. Sorting yielded a homogeneous CAR-positive population that was used for all downstream experiments.

Cytotoxicity assay

The *in vitro* cytotoxic activity of YTS eco cells against various target cells was assessed either by Calcein-AM-labeled target cells (ThermoFisher Scientific, cat. no. C1430) or FACS. Although the absolute levels of cytotoxicity were not identical across methods, they provided a reliable basis for comparison between the various cell platforms. Cytotoxicity was evaluated at multiple time points, including 3, 24, and 48 hours, depending on the specific experiment. For the Calcein-AM assay, target cells (3×10^6) were counted, washed with RPMI, and resuspended in Calcein-AM (1 mg/mL) diluted at a 1:200 ratio. The cells were then incubated at 37°C for 30 minutes, centrifuged, washed with RPMI, and resuspended in RPMI+. Ten thousand cells were plated per well in a 96-well U-bottom plate. For standard cytotoxicity assays, target cells were resuspended in 100 µL RPMI+. For ADCC experiments, target cells were resuspended in 50 µL RPMI+, incubated with antibodies at 0.5 µg/well (in 50 µL volume) for 1 hour on ice, and then mixed with YTS cells at a predetermined effector-to-target (E: T) ratio in an additional 100 µL. For CD28 blocking, YTS cells were pre-incubated with 0.5 µg of anti-CD28 antibody (clone L293, BD Biosciences, cat. no. 348040) for 1 hour on ice. Each experiment was performed in quadruplicate. Plates were incubated at 37°C for 3 hours,

centrifuged, and 100 µL of the supernatant was transferred to black, flat-bottom 96-well plates (Greiner) for fluorescence measurement using either a Tecan plate reader or a GloMax Explorer (Promega). Spontaneous release controls contained target cells incubated in medium only, and maximum lysis controls were treated with 50 nM NaOH. Percent specific lysis was calculated using the formula: % Cytotoxicity = [(experimental release – spontaneous release) / (maximum release – spontaneous release)] × 100.

For assessment of cytotoxicity by flow cytometry, YTS CAR-CD19 (1×10^6 cells/mL) were co-cultured with Raji target (1×10^5 cells/mL) at an E:T ratio of 10:1 for 3 hours at 37°C. Following incubation, cells were collected and stained with Zombie NIR viability dye (diluted 1:1000), then with anti-CD19 (APC) and anti-CD56 (PE) antibodies (diluted 1:200). Live cell counts were normalized to control wells, which contained target cells alone in medium.

Production of CAR T cells and NK-92 CAR

We cloned CAR-CD19 with a CD28 costimulatory domain into an MSCV retroviral vector with puromycin resistance, adding an N-terminal FLAG tag. Retroviral particles were initially produced using EcoPhoenix cells, and the resulting supernatant was used to transduce PG13 cells. Puromycin-resistant PG13 clones were selected using puromycin (InvivoGen), establishing stable producers of the retrovirus. Peripheral blood mononuclear cells (PBMCs) were isolated from a healthy donor by Ficoll density gradient centrifugation, and stimulated for 48 hours with anti-CD3 (50 ng/mL, Miltenyi Biotec) and IL-2 (300 IU/mL, Novartis). Subsequently, PBMCs were transduced with viral supernatant collected from the PG13 producer cells. Transduction efficiency was confirmed by FACS, with approximately 50% of cells expressing the CAR. The same retroviral system was used to transduce NK-92 cells to generate NK-92 CAR cells. In parallel, the identical FLAG-tagged CAR sequence was cloned into a lentiviral vector and used to generate YTS-CAR CD19 FLAG cells, as described in the

main Methods section. CAR-positive NK-92 CAR and YTS-CAR cells were enriched using anti-FLAG magnetic selection. Briefly, cells were incubated with anti-FLAG antibody (BioLegend, cat. no. 637323) followed by magnetic labeling and separation using the Miltenyi Biotec system (cat. no. 130-042-401) according to the manufacturer's instructions.

Cell Irradiation and Assessment of Cell Proliferation

Cells were irradiated at varying doses using the MultiRad 350 X-ray irradiator (Precision X-Ray). To assess the effects of irradiation on cell proliferation and viability, we employed the following methods:

Thiazolyl Blue Tetrazolium Bromide (MTT) assay

Fifty milligrams of MTT (Sigma-Aldrich) were dissolved in 10 mL of 1× PBS (Biological Industries) and filtered using a 0.22 μm filter (Millipore). Cells were counted and plated at a density of 3×10^5 cells/mL. They were then exposed to escalating doses of irradiation: 1000, 2000, 3000, and 6000 rad. Each day, 100 μL of cell suspension was transferred into 96-well U-bottom plates, followed by the addition of 10 μL MTT stock solution per well. The plate was gently mixed by pipetting and incubated at 37°C for 3 hours. After incubation, the plate was centrifuged at 1600 rpm for 5 minutes to pellet the cells, and the medium was carefully removed. DMSO (100 μL) was added to each well, and the cells were thoroughly resuspended. The plate was then incubated at 37°C for 10 minutes, and 90 μL of each well's contents was transferred to flat-bottom 96-well plates. Absorbance was measured at 490 nm using a microplate reader (BioTek).

CellTrace proliferation assay

Fifteen million cells (1.5×10^7) were stained with 0.2 µM CellTrace™ Far Red Cell Proliferation dye (Invitrogen) in a total volume of 1.5 mL, following the manufacturer's instructions. Stained cells were diluted to a final concentration of 3×10^5 cells/mL and irradiated at 1000, 2000, 3000, and 6000 rad. Daily, 500 µL samples were collected and fixed in 1% paraformaldehyde (PFA). Samples were analyzed on the same day using a DxFLEX Flow Cytometer (Beckman Coulter).

Viability testing

Cell viability was assessed using the Zombie NIR™ Fixable Viability Kit (BioLegend), according to the manufacturer's protocol. Cells were counted and diluted to 3×10^5 cells/mL, then exposed to the same irradiation doses: 1000, 2000, 3000, and 6000 rad. Each day, 200 µL of the culture was transferred to 96-well U-bottom plates and stained with the viability dye at 1:1000 dilution. All samples were analyzed on the same day using the DxFLEX Flow Cytometer (Beckman Coulter).

IFN-γ ELISA

IFN-γ secretion was quantified using a sandwich ELISA with a biotin–streptavidin–HRP detection system. ELISA plates were coated overnight at 4°C with anti–IFN-γ capture antibody (0.2 µg/ml, BioLegend, cat. no. 502402), washed with 0.05% Tween 20 in phosphate-buffered saline (PBST), and blocked with 1% BSA for 2 hours at 37°C. NK-92 or YTS expressing CAR CD19 effector cells were co-cultured with Raji target cells at an effector-to-target ratio of 5:1 for 24 hours, after which supernatants were collected and centrifuged. Supernatants (200 µl/well) were added to the plates and incubated for 2 hours at 37°C. Plates were then incubated with biotinylated anti–IFN-γ detection antibody (0.1 µg/ml, BioLegend, cat. no. 502504) for 1 hour at room temperature, followed by streptavidin–HRP for 30 minutes. Signal was developed

using TMB substrate, and absorbance was measured at 450 nm using a GloMax microplate reader. Experiments were performed independently four times.

EBV Transfer assessment

To assess EBV transfer, YTS-CAR CD19 cells were added to HEK293T cells at an effector-to-target ratio of 5:1 and co-cultured for 24 hours at 37°C. Following incubation, non-adherent YTS cells were removed by repeated PBS washes, and the remaining adherent HEK293T cells were cultured in fresh medium for an additional 5 days at 37°C. Total genomic DNA was then extracted from the HEK293T cells using the DNeasy Blood & Tissue Kit (Qiagen, cat. no. 69504) according to the manufacturer's instructions. The presence of EBV DNA was assessed by qPCR using primers specific for the BALF5 gene.

Knockout of 2B4

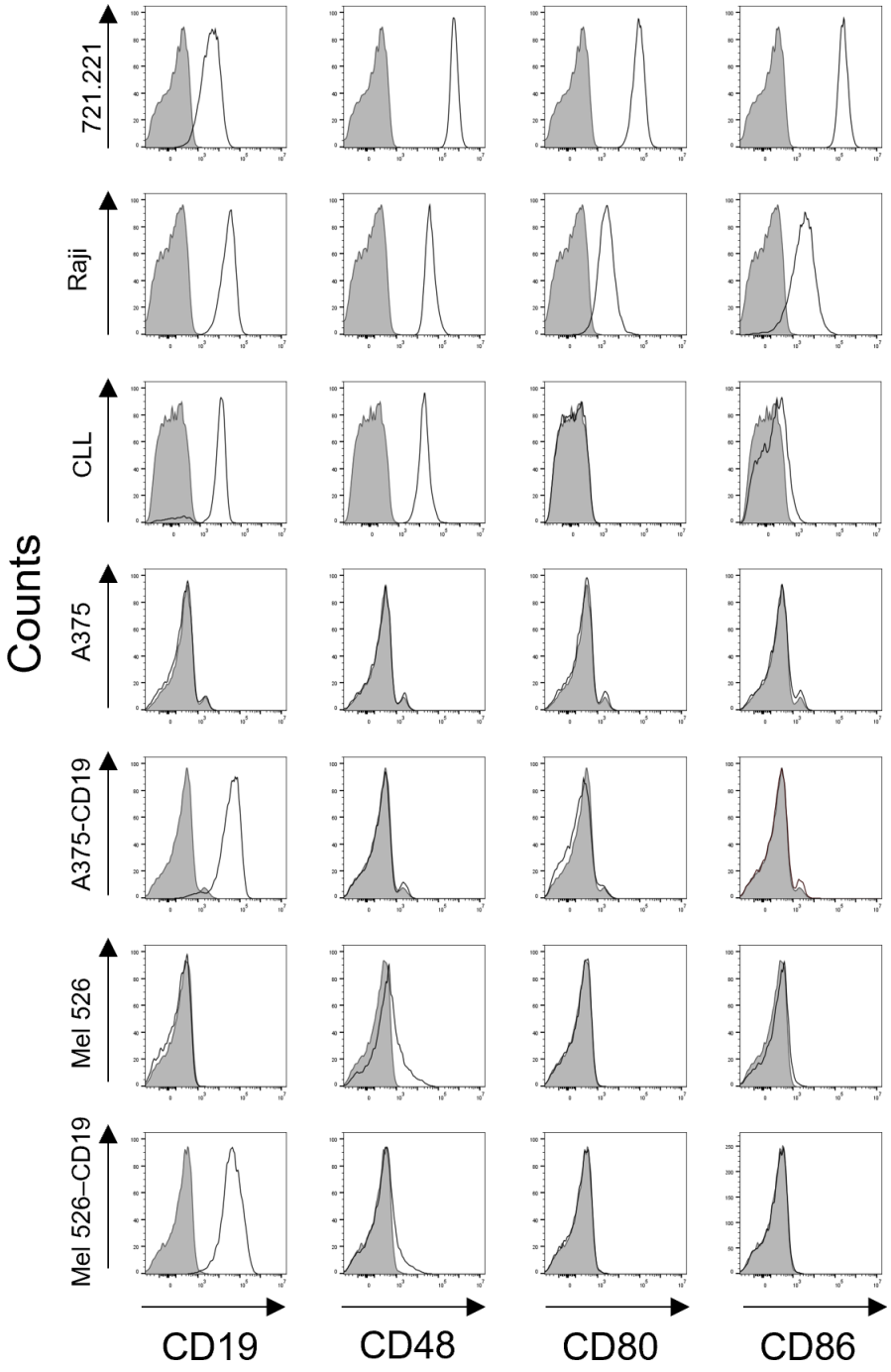
gRNA targeting the 2B4 receptor (CD244) (5'-CACCGCTGCTCCTCAAGGTGTATCA-3') was cloned into the lentiGuide-Puro plasmid (Addgene #52963) using Esp3I, transformed into E. coli, and verified by Sanger sequencing. Plasmid DNA was purified using the ZymoPURE II Maxiprep Kit. Lentivirus was produced by transfecting HEK293T cells (1.25×10^6 cells/well) with the gRNA plasmid, psPAX2 (Addgene #12260), and pCMV-VSV-G (Addgene #8454) using TransIT-LT1. Viral supernatant was collected 48 hours later, filtered, and stored. Cas9-expressing YTS cells (5×10^5 cells/mL), generated in-house, were infected with the virus in the presence of 6 μg/mL polybrene, followed by spinfection (1,800 rpm, 90 min, RT). Medium was replaced two days post-infection.

Dendritic cell extraction

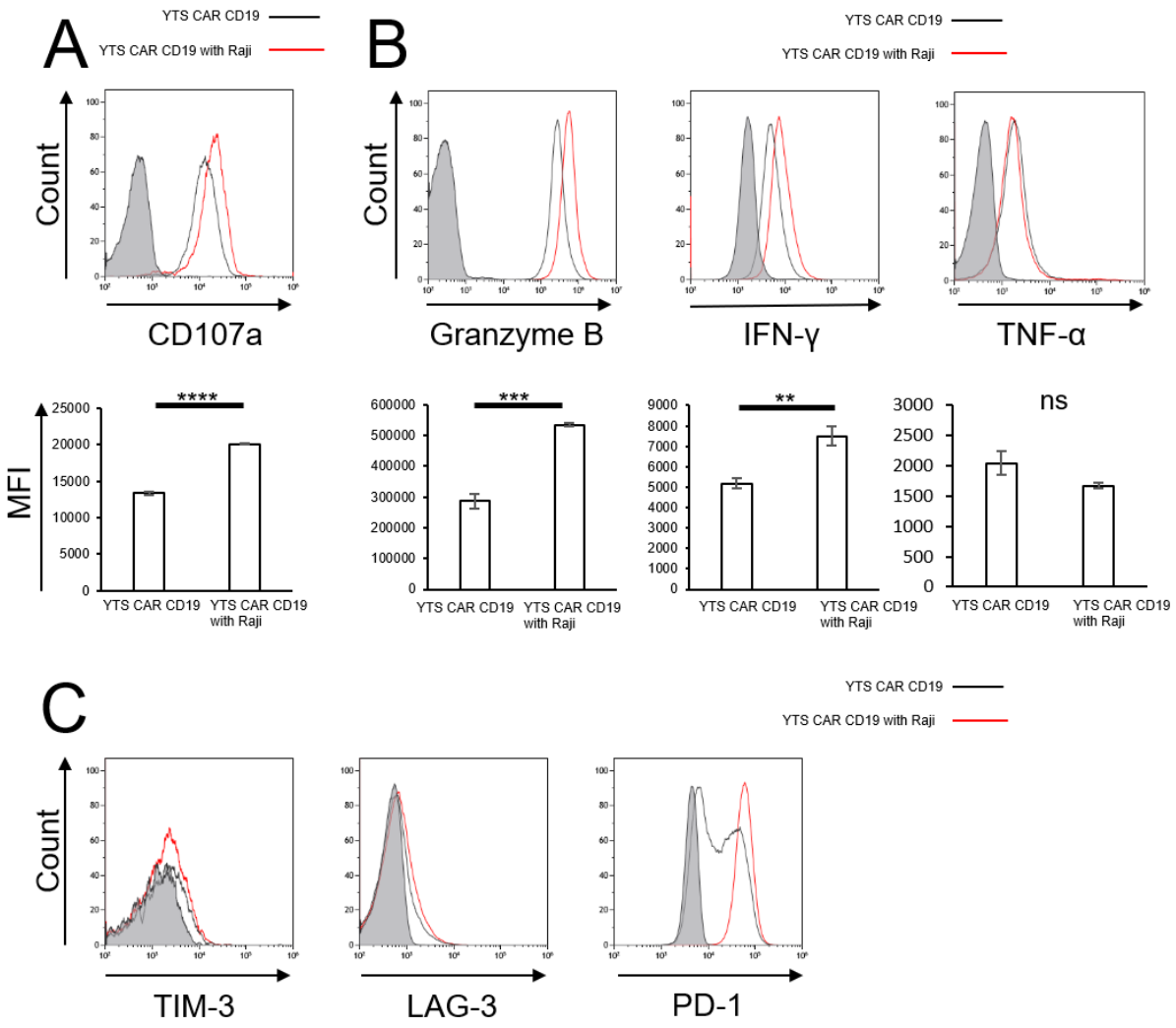
Monocyte-derived dendritic cells (DCs) were generated from peripheral blood mononuclear cells (PBMCs) collected from a healthy donor. PBMCs were washed, seeded in 35 mm culture plates, and incubated at 37°C with 5% CO2 to allow monocyte adherence. Non-adherent cells

were removed, and monocytes were cultured in media containing 1% autologous plasma, 1,000 U/mL GM-CSF, and 1,000 U/mL IL-4. Every 2 days, 0.25 mL of media was replaced with 0.35 mL of fresh media containing plasma, GM-CSF (500 U/mL), and IL-4 (500 U/mL). On day 6, immature DCs were harvested by trypsinization and scraping. To generate mature DCs, on day 6, cells were stimulated with 10 ng/mL LPS and incubated for an additional 24 hours. Morphological changes (increased size and pseudopods) confirmed activation. Cells were then detached using trypsin-EDTA and scraped for further analysis.

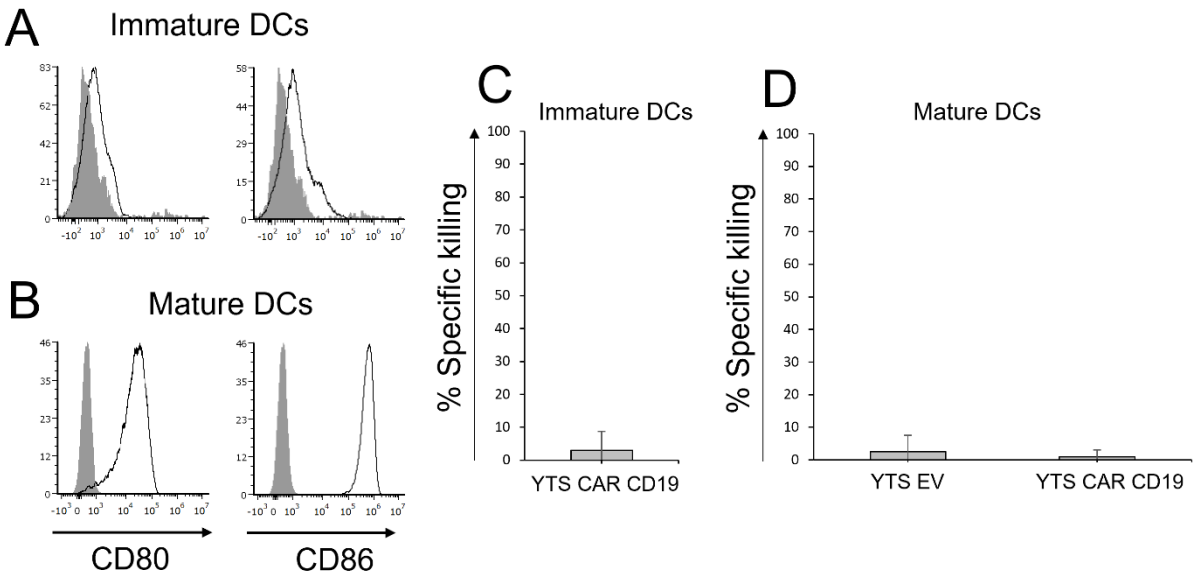
Supplementary Figures



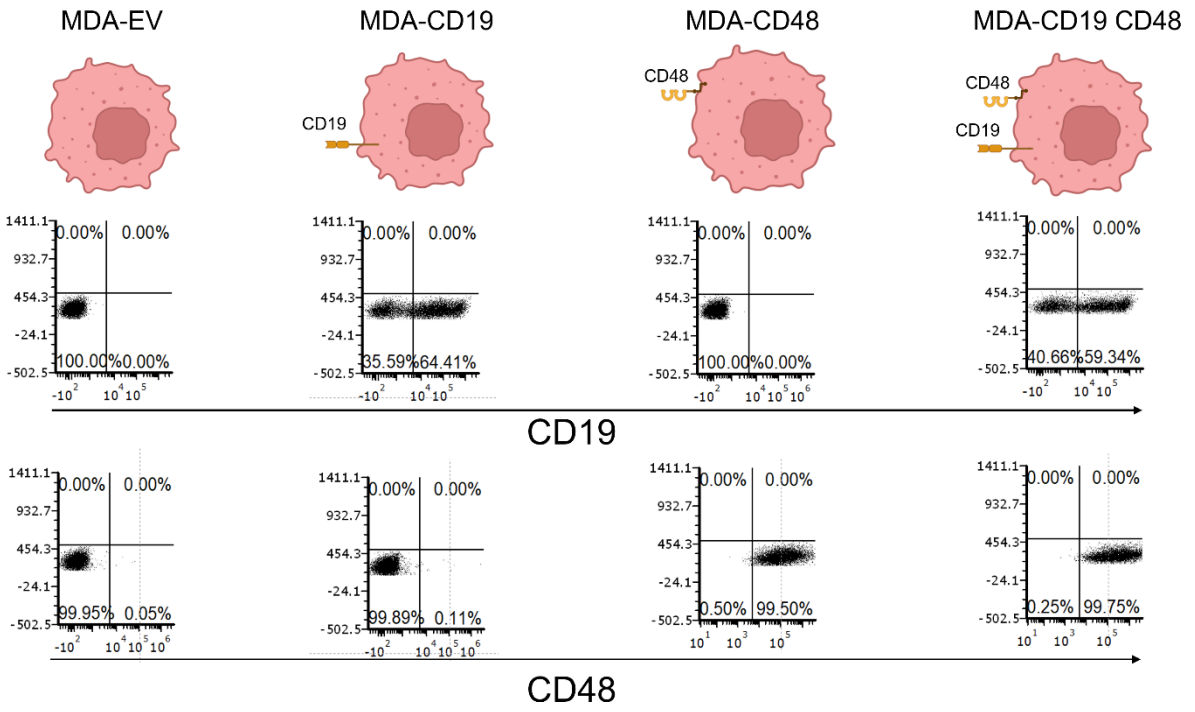
Supplementary Figure 1. Flow cytometry analysis of CD19, CD48, CD80, and CD86 expression across various cell lines. Data shown are representative of two independent experiments.



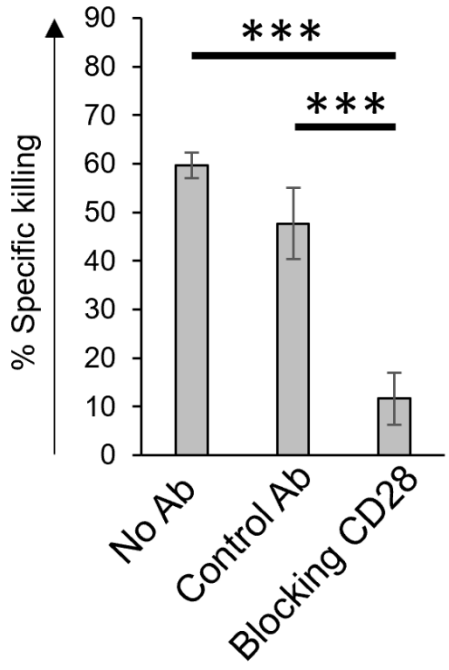
Supplementary Figure 2. Intracellular cytokine, cytotoxic molecule, and exhaustion marker staining of YTS-CAR CD19 cells. YTS-CAR CD19 cells were analyzed in the presence or absence of Raji target cells for CD107a expression (A), intracellular granzyme B and cytokine production (B), and exhaustion marker expression (C). Effector-to-target (E:T) ratios were 10:1 for panel A and 20:1 for panels B and C. Panels A and B were performed in triplicate. Data shown are from one representative experiment out of two performed. ** P< 0.01, *** P < 0.001, **** < P 0.0001, Student's *t*-test.



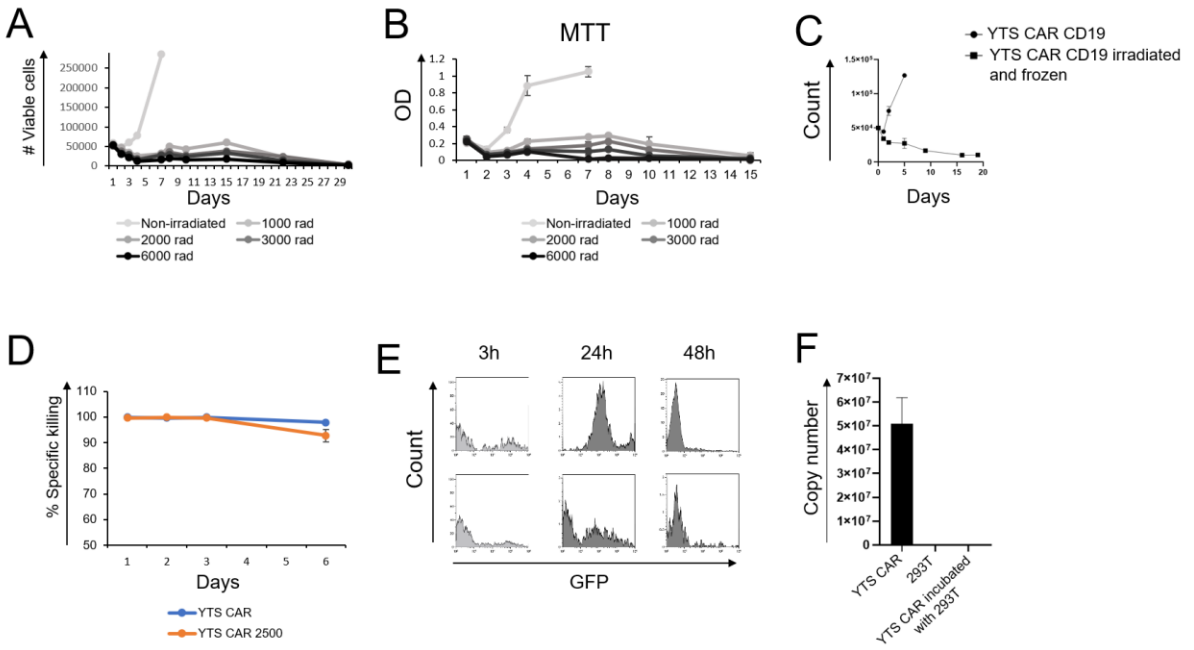
Supplementary Figure 3. Cytotoxicity of YTS cells against dendritic cells. (A, B) FACS analysis of CD80 and CD86 expression in immature (A) and mature (B) dendritic cells. (C, D) Cytotoxicity assays using Calcein-AM–labeled immature (C) and mature (D) dendritic cells co-cultured with YTS cells expressing either an empty vector or a CD19-specific CAR. Effector-to-target (E:T) ratio was 20:1.



Supplementary Figure 4. Transfectants of MDA-MB-453 cells expressing CD19 and CD48. FACS analysis of MDA-MB-453 cells showing expression of CD19, CD48, or both. Illustrations in the top row were created with BioRender.com.

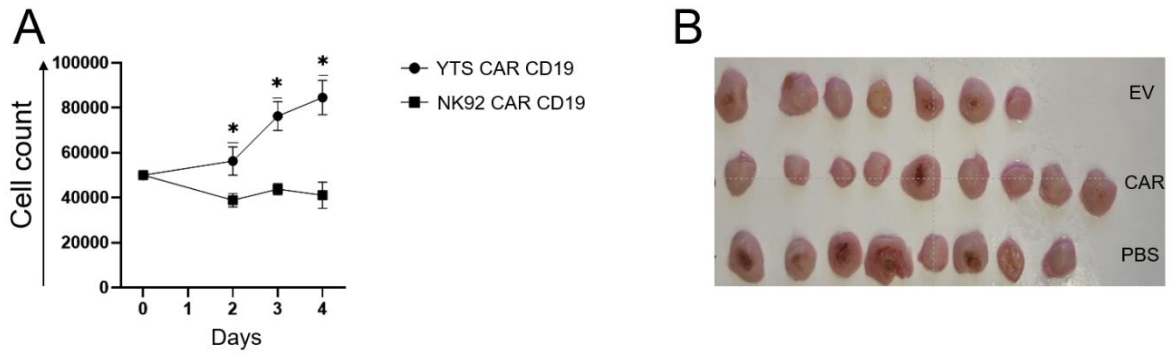


Supplementary Figure 5. Cytotoxicity of CAR-expressing YTS cells against 721.221 cells with CD28 blockade. YTS cells expressing a CD19-specific CAR were pre-incubated with either a control antibody or an anti-CD28 antibody, then co-cultured with Calcein-AM–labeled 721.221 cells at an effector-to-target (E:T) ratio of 20:1. The experiment was repeated two times and performed in six replicates. *** $P < 0.001$, Student's *t*-test.



Supplementary Figure 6. Safety of irradiated YTS-CAR cells. (A,B) YTS cells expressing a CD19-targeted CAR were either left non-irradiated or irradiated at the indicated doses and subsequently assessed for viability and metabolic activity. (A) Viable cells were quantified by flow cytometry for up to 30 days. (B) Metabolic activity was evaluated using an MTT assay for up to 15 days. Follow-up of non-irradiated cells was limited to day 7, as the culture medium was not replenished. (C) Irradiated and frozen YTS-CAR cell numbers were monitored up to 20 days by flow cytometry using viability gating. Fresh non-irradiated cells were used as control. (D) Cytotoxic activity of YTS-CAR CD19 cells over time. The cytotoxic activity of frozen-thawed, irradiated or non-irradiated YTS FLAG-CAR CD19 cells was assessed against Raji target cells at different time points (E:T ratio = 10:1) using a flow cytometry–based killing assay. The experiment was repeated twice. A complementary cytotoxicity assay using Calcein-AM labeling was also performed and showed similar trends. **(**E**)** *In vivo* persistence of irradiated YTS-CAR CD19 cells. 20X10^6 irradiated and frozen YTS-CAR CD19 cells were injected into NSG mice, and their presence in peripheral blood was analyzed by flow cytometry at different time points after infusion. Data are shown for five individual mice at the indicated time points. (F) EBV transfer assessment: HEK293T cells were co-cultured with YTS-CAR

CD19 cells at an effector-to-target ratio of 5:1 for 24 h, followed by removal of YTS cells. After 5 days, genomic DNA was extracted from HEK293T cells and EBV presence was assessed by qPCR targeting BALF5.



Supplementary Figure 7. Comparison of YTS-CAR and NK-92 CAR proliferation and representative tumor images from an *in vivo* experiment. (A) Comparison of proliferation of YTS-CAR and NK-92 CAR cells. YTS-CAR and NK-92 CAR cells were seeded at equal densities ($0.5X10^6$ cells/mL) and monitored over time by flow cytometry using viability staining. Data shown are from one representative experiment out of two performed, each conducted in triplicate. (B) Representative images of tumors collected from the experiment shown in Figure 5B.